Random Receiver Orientation Effect on Channel Gain in LiFi Systems

Citation for published version:
Dehghani Soltani, M, Zeng, Z, Tavakkolnia, I, Haas, H & Safari, M 2019, Random Receiver Orientation Effect on Channel Gain in LiFi Systems. in *IEEE Wireless Communications and Networking .* IEEE Wireless Communications and Networking Conference, Marrakech, Morocco, 15/04/19.
https://doi.org/10.1109/WCNC.2019.8886097

Digital Object Identifier (DOI):
10.1109/WCNC.2019.8886097

Link:
Link to publication record in Edinburgh Research Explorer

Document Version:
Peer reviewed version

Published In:
IEEE Wireless Communications and Networking

Random Receiver Orientation Effect on Channel Gain in LiFi Systems

Mohammad Dehghani Soltani, Zhihong Zeng, Iman Tavakkolnia, Harald Haas, Majid Safari
LiFi R&D Center, Institute for Digital Communications, School of Engineering, The University of Edinburgh, UK
Email: {m.dehghani, zhihong.zeng, i.tavakkolnia, h.haas, majid.safari}@ed.ac.uk

***Abstract*—Light-Fidelity (LiFi) has been considered as a complementary technology to radio frequency (RF) communications. The reliability of a LiFi channel highly depends on the availability and alignment of line-of-sight (LOS) links. In this study, we investigate the effect of receiver orientation including both polar and azimuth angles on the LOS channel gain in a LiFi system. The optimum tilt angle is calculated, which depends on both the user's location and direction. The probability density function (PDF) of signal-to-noise ratio (SNR) is derived for on-off keying (OOK) modulation. Using the derived PDF of SNR, the bit-error ratio (BER) of OOK in an additive-white Gaussian noise (AWGN) channel with random orientation of the receiver is evaluated. It is shown that the effect of random orientation is negligible if the optimum tilt angle is chosen. Finally, we assess the effect of random orientation on the Shannon-Hartley upper bound capacity.**

***Index Terms*—Random orientation, bit-error ratio (BER), light-fidelity (LiFi).**

I. INTRODUCTION

It is anticipated that mobile data traffic will generate about 49 exabyte per month and the average global mobile connection speed will surpass 20 Mbps by 2021 [1]. The total number of smartphones (including phablets) will be over 50% of global devices and they will generate more than 86% of mobile data traffic by 2021 [1]. Therefore, both academia and industry are looking for alternative solutions to offload heavy traffic loads from radio frequency (RF) wireless networks. Light-Fidelity (LiFi) is a novel bidirectional, high-speed and fully networked wireless communication system that utilizes visible light and infrared in the downlink and uplink transmission, respectively [2]. Compared to RF networks, LiFi offers notable benefits such as providing enhanced security, utilizing a very large and unregulated bandwidth and energy efficiency. These advantages have put LiFi in the scope of recent and future research.

Device orientation can remarkably affect the users' throughput. The majority of studies on optical wireless communications assume that the device always faces vertically upwards. Although this may be for the purpose of analysis simplification or due to lack of a proper model for device orientation, in a real life scenario users hold their device in a way that feels most comfortable. This can mean that the device is not always facing upwards and can have any random orientation. However, some studies have considered the impact of random orientation in their analysis [3]–[15]. Device orientation can be measured by the gyroscope and accelerator embedded in every smartphone. Then, this information can be fed back to the access point (AP) by a limited-feedback scheme to enhance the system performance [16]–[18].

An AP selection algorithm for randomly-orientated UEs in LiFi networks is proposed in [3]. The orientation of UEs is modeled based on the Euler's rotation theorem and using the rotation about each axis. By employing the same modeling for UE's orientation, the handover probability and rate is evaluated in a standalone LiFi network with the consideration of random orientation and mobility of UEs in [4]. In [5], the handover probability is evaluated in a hybrid LiFi/RF-based network. The impact of the receiver tilt angle on channel capacity in visible light communication systems is shown in [6]. It is expressed that by properly tilting the receiver plane the channel capacity can be improved dramatically. The same approach is used in [7] to enhance the bit-error ratio (BER) of the on-off keying (OOK) modulation. In [8], the Newton method is employed to find the optimum tilt angle. By properly tilting the PD plane according to this optimum tilt angle, the signal-to-noise ratio (SNR) and spectral efficiency of M-QAM orthogonal frequency division multiplexing (OFDM) are enhanced. The optimum tilt angle of each PD for a single user multiple-input multiple output (MIMO) is obtained in [9]. It is shown that the cross-correlation of line-of-sight (LOS) channel gains at each PD is reduced. The impact of random orientation on LOS channel gain for randomly located users is investigated in [10]. The statistical channel gain is derived under the assumption of a Gaussian model for the polar angle. It is noted that none of these studies are supported by any experimental data. A more realistic model for the polar angle based on the experimental measurements is considered in [14]. Using this model, the impact of random orientation on BER of a DC biased optical OFDM (DCO-OFDM) as a use case is evaluated. Measurements and modeling of random orientations of cellphones are reported in [11]–[13]. It is shown that the probability density function (PDF) of the polar angle can be modeled as a Laplace distribution for sitting activities and a Gaussian distribution for walking activities [13]. All these works signify the importance of incorporating device orientation. In [15], the impact of random orientation on a multi-directional receiver using spatial modulation is studied.

In this study, we evaluate the impact of device orientation on the LOS channel gain. Then, we provide a closed form solution for the optimum tilt angle. The effect of narrow and wide field-of-view (FOV) on the LOS performance is assessed. It should be noted that both [6] and [7] study the

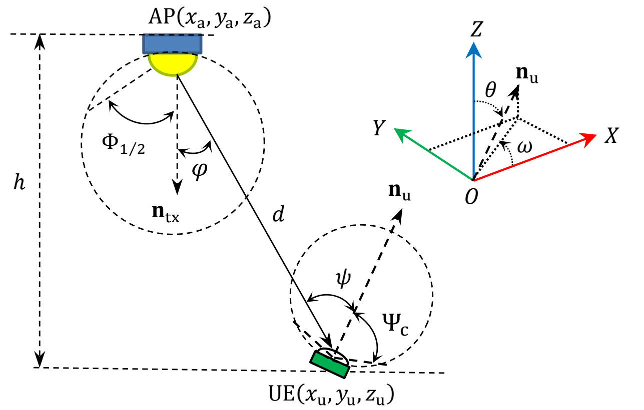

Fig. 1: Downlink geometry of LOS link in LiFi systems.

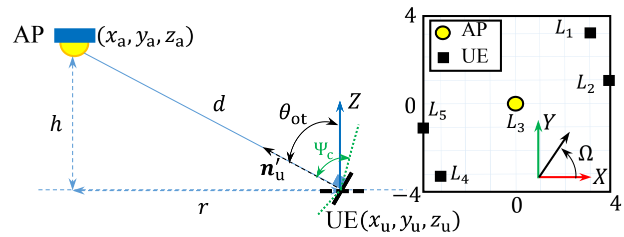

Fig. 2: Geometry of optimum tilt angle and considered positions in the room.

effect of the tilt angle without considering the impact of the random orientation on BER and link capacity. Furthermore, an optimization problem is formulated in their studies to find the optimum tilt angle. We also derive the PDF of SNR for OOK modulation with the consideration of random orientation. Using the derived PDF of SNR, the BER of OOK modulation and upper bound capacity are evaluated.

II. System Model

The downlink geometry of the LOS link in a LiFi system is represented in Fig. 1. The direct current (DC) gain of the LOS optical wireless channel between the AP and the UE can be obtained as [19]:

$$H = \frac{(m+1)A_{\rm PD}}{2\pi d^2} g_{\rm f} \cos^m \phi \cos\psi \;{\rm rect}\left(\frac{\psi}{\Psi_{\rm c}}\right), \qquad (1)$$

where $A_{\rm PD}$ is the physical area of the photodetector (PD); the Lambertian order is $m = -1/\log_2(\cos\Phi_{1/2})$ and $\Phi_{1/2}$ denotes the transmitter semiangle at half power. The Euclidean distance between the AP location, $(x_{\rm a}, y_{\rm a}, z_{\rm a})$, and the UE location, $(x_{\rm u}, y_{\rm u}, z_{\rm u})$, is shown by d. The gain of the optical concentrator is denoted by $g_{\rm f} = \varsigma^2/\sin^2\Psi_{\rm c}$ with ς being the refractive index and $\Psi_{\rm c}$ is the UE field of view (FOV). The incidence angle with respect to the normal vector to the UE surface, $\mathbf{n}_{\rm u}$, and the radiance angle with respect to the normal vector to the AP surface, $\mathbf{n}_{\rm tx} = [0, 0, -1]$, are denoted by ϕ and ψ, respectively. These two angles can be obtained using the analytical geometry rules as $\cos\phi = \mathbf{d}\cdot\mathbf{n}_{\rm tx}/d$ and $\cos\psi = -\mathbf{d}\cdot\mathbf{n}_{\rm u}/d$ where $\mathbf{d}$ is the distance vector from the AP to the UE and $\cdot$ is the inner product operator. Furthermore, ${\rm rect}(\frac{\psi}{\Psi_{\rm c}}) = 1$ for $0 \le \psi \le \Psi_{\rm c}$ and 0 otherwise. After some manipulations, (1) can be simplified as:

$$H = \frac{H_0 \cos\psi}{d^{m+2}} \;{\rm rect}\left(\frac{\psi}{\Psi_{\rm c}}\right), \qquad (2)$$

where $H_0 = \frac{(m+1)A_{\rm PD} g_{\rm f} h^m}{2\pi}$; and $h = |z_{\rm a} - z_{\rm u}|$ denotes the vertical distance between the AP and the UE as represented in Fig. 1. Note that in the spherical coordinate system the normal vector $\mathbf{n}_{\rm u}$ can be represented in terms of the polar angle, θ, and the azimuth angle, ω, (as shown in subset of Fig. 1). Therefore, $\cos\psi$ can be expressed as [14]:

$$\begin{aligned}\cos\psi &= \lambda_1 \sin\theta + \lambda_2 \cos\theta \\ &= \sqrt{\lambda_1^2 + \lambda_2^2}\cos\left(\theta - \tan^{-1}\left(\frac{\lambda_1}{\lambda_2}\right)\right),\end{aligned} \qquad (3)$$

where λ_1 and λ_2 are given as:

$$\begin{aligned}\lambda_1 &= \frac{r}{d}\cos\left(\Omega - \tan^{-1}\left(\frac{y_{\rm u} - y_{\rm a}}{x_{\rm u} - x_{\rm a}}\right)\right), \\ \lambda_2 &= \frac{h}{d}.\end{aligned} \qquad (4)$$

where $r = \sqrt{(x_{\rm u} - x_{\rm a})^2 + (y_{\rm u} - y_{\rm a})^2}$ is the horizontal distance between the AP and the UE.

It is reported in [13] and [20] that the polar angle can be modeled as a Laplace distribution, $\theta \sim \mathcal{L}(\mu_\theta, b_\theta)$, where μ_θ and $b_\theta = \sigma_\theta/\sqrt{2}$ denote the mean value and scale parameter, respectively. These values are reported in [13] for static and mobile users. Moreover, it is shown that the azimuth angle can be modeled as a uniform distribution, $\omega \sim \mathcal{U}[0, 2\pi]$. The angle of the direction that the user is facing is defined as $\Omega = \omega + \pi$. In fact, Ω gives a better physical concept (compared to ω), as it denotes the angle between the user's facing direction and the X-axis.

III. Orientation Analysis and its Impact on The LOS Link

In this section, we evaluate the effect of θ and Ω on the LOS channel gain. According to [12], [13], [20], we assume that $\theta \in [0°, 90°]$. Referring to (2), for a given location of UE, the LOS DC gain is maximum when $\cos\psi$ is maximum. It takes its highest value when $\Omega = \tan^{-1}\left(\frac{y_{\rm u} - y_{\rm a}}{x_{\rm u} - x_{\rm a}}\right) \triangleq \Omega_{\rm ot}$ and

$$\theta = \cos^{-1}\left(\frac{h}{d}\right) \triangleq \theta_{\rm ot}, \qquad (5)$$

where $\theta_{\rm ot}$ is the optimum tilt angle. In fact, the optimum tilt angle is the polar angle for which $\psi = 0$ (or the LOS channel gain is maximum) as shown in Fig. 2. For any arbitrary location of the UE and a given $\Omega \in \mathcal{R}_\Omega$, the optimum tilt angle can be obtained as:

$$\begin{aligned}\theta_{{\rm ot},\Omega} &= \arg\max_\theta \cos\psi \\ &= \arg\max_\theta \sqrt{\lambda_1^2 + \lambda_2^2}\cos\left(\theta - \tan^{-1}\left(\frac{\lambda_1}{\lambda_2}\right)\right) \\ &= \tan^{-1}\left(\frac{\lambda_1}{\lambda_2}\right),\end{aligned} \qquad (6)$$

and for $\Omega \notin \mathcal{R}_\Omega$, $\theta_{\rm ot} = 0$; where $\mathcal{R}_\Omega$ defines the range of Ω for which the AP is in the FOV of the UE.

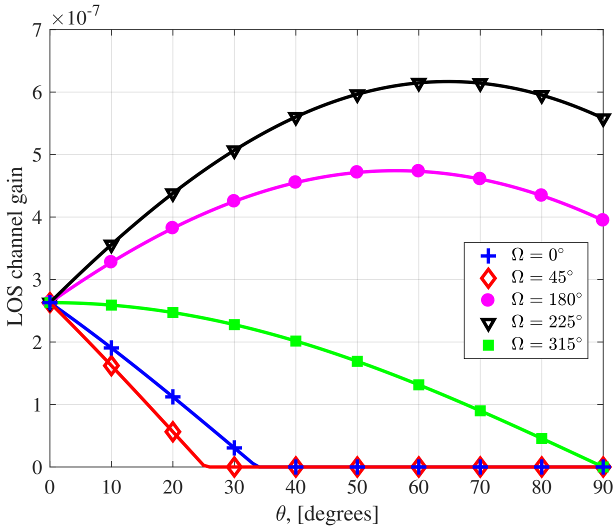

Fig. 3: The effect of changing Ω and θ on the LOS channel gain with $\Psi_c = 90°$, for the given position of L_4.

For the given location of L_4 (shown in the subset of Fig. 2) and with $\Psi_c = 90°$, Fig. 3 shows the curves of the LOS channel gain versus θ for various values of Ω. Other simulation parameters are given in Table I. It can be seen that for the given location based on the angle Ω, we have different values for the optimum tilt angle that can be determined according to (6). For instance, for $\Omega = 180°$, we have $\theta_{\text{ot},\Omega} = 56°$ and for $\Omega = 225°$, we have $\theta_{\text{ot}} = 65°$. For directions of $0°$, $45°$ and $315°$ the optimum tilt angle is $0°$ (or vertically upward). For any $\Omega \in \mathcal{R}_\Omega = [135°, 315°]$, the optimum tilt angle can be obtained by (6). While for Ω out of $\mathcal{R}_\Omega$, the optimum tilt angle is $\theta_{\text{ot}} = 0°$. It should be noted that under the condition of $\Omega = \Omega_{\text{ot}}$ and $\theta = \theta_{\text{ot}}$ given in (5), the maximum LOS channel gain can be achieved.

The optimum tilt angles for the locations of L_1 and L_2 with $\Omega = 45°$ equal to $64.76°$ and $60.5°$, respectively. However, for the locations of L_4 and L_5 with $\Omega = 45$, the optimum tilt angle is zero. It is also intuitive that when the UE faces toward the AP, there exists an optimum θ that results in the maximum LOS channel gain. However, if the UE faces in the opposite direction of the AP, then, $\theta = 0°$ leads to the maximum value for the channel gain. As can be noticed from (6), the optimum tilt angle depends on the UE's location and its direction and it is independent of the FOV. In the following, we investigate the effect of FOV on the LOS channel gain.

For a given Ω and UE's position, let's define $\Psi_{\Omega,\min}$ as the minimum FOV for which if $\Psi_c \le \Psi_{\Omega,\min}$ then the LOS channel gain is zero for any $\theta \in [0°, 90°]$. This minimum FOV is given as:

$$\Psi_{\Omega,\min} = \cos^{-1}\left(\sqrt{\lambda_1^2 + \lambda_2^2}\right). \tag{7}$$

From (3), we have $\cos\psi = \sqrt{\lambda_1^2 + \lambda_2^2}\cos\left(\theta - \tan^{-1}\left(\frac{\lambda_1}{\lambda_2}\right)\right)$. For a given UE's location and Ω, for any $\theta \in [0°, 90°]$, $\cos\psi \le \sqrt{\lambda_1^2 + \lambda_2^2}$. On the other hand, if $\cos\psi \le \cos\Psi_c$, the LOS channel gain is zero. Consequently, for $\Psi_c \le \cos^{-1}(\sqrt{\lambda_1^2 + \lambda_2^2}) \triangleq \Psi_{\Omega,\min}$, the LOS channel gain is always zero. The physical concept of $\Psi_{\Omega,\min}$ is that for a given UE's location and Ω, with $\Psi_c \le \Psi_{\Omega,\min}$, the AP is always out of the UE's FOV for all $\theta \in [0°, 90°]$.

TABLE I: Simulation Parameters

Parameter	Symbol	Value
Receiver FOV	Ψ_c	$90°$
LED half-intensity angle	$\Phi_{1/2}$	$60°$
PD responsivity	R_{PD}	1 A/W
Physical area of a PD	A	1 cm^2
Transmitted electrical power	P_{elec}	1 W
Downlink bandwidth	B	10 MHz
Noise power spectral density	N_0	10^{-21} A^2/Hz
Vertical distance of UE and AP	h	2 m

Fig. 4-(a) illustrates the impact of different FOVs on the LOS channel gain versus θ for L_1 and L_5 with $\Omega = 45°$. It can be observed that the UE's FOV affects the LOS channel gain remarkably. As it can be seen, narrower FOV results in a smaller range of θ for which the LOS channel gain is non-zero. In other words, the user is able to tilt the device more without missing the LOS link. Furthermore, it can be noticed that if the UE is located at L_5 it is more greatly affected by the reduction of the FOV compared to the position L_1. Based on (7), the minimum FOV that ensures the visibility of LOS link for these two locations, L_5 and L_1, are $\Psi_{\Omega,\min} = 64.12°$ and $\Psi_{\Omega,\min} = 1°$, respectively. This means that for the location of L_5 and $\Omega = 45°$, with $\Psi_c \le 64.12°$, the LOS channel gain is out of the UE's FOV for all $\theta \in [0°, 90°]$. Therefore, in order to guarantee the visibility of the AP in the UE's FOV, the condition $\Psi_c \ge \Psi_{\Omega,\min}$ should be fulfilled. However, for the location of L_1 and $\Omega = 45°$, a narrow FOV can guarantee the visibility of AP for all polar angles of $\theta \in [0°, 90°]$. This can be considered as one important metric in design of FOV to mitigate co-channel interference.

For a given θ and UE's position, let's define $\Psi_{\theta,\min}$ as the minimum FOV for which if $\Psi_c \le \Psi_{\theta,\min}$ then LOS channel gain is zero. This $\Psi_{\theta,\min}$ is given as:

$$\Psi_{\theta,\min} = \cos^{-1}(\kappa_1 + \kappa_2) = |\tan^{-1}\left(\frac{r}{h}\right) - \theta|. \tag{8}$$

Detailed proof of (8) is provided in Appendix A. To better understand the physical concept of $\Psi_{\theta,\min}$, consider the case with $\theta = 0$ (vertically upward device), the minimum FOV that ensures non-zero LOS channel gain at any arbitrary location is $\Psi_{\theta,\min} = \tan^{-1}\left(\frac{r}{h}\right)$. In other words, if Ψ_c is less than $\Psi_{\theta,\min}$, the LOS channel gain is zero. The effect of different FOV on the LOS channel gain versus Ω for L_1 and L_5 with $\theta = 41°$ (this value is reported in [13] as the mean of experimental data for sitting users) are shown in Fig. 4-(b). According to (8), the smallest FOV for which the LOS channel gain is still non-zero would be $\Psi_{\theta,\min} = 23.12°$ for L_5 and $\Psi_{\theta,\min} = 23.76°$ for L_1. This can be confirmed from the results shown in Fig. 4-(b) where for $\Psi_c = 24°$, the LOS channel gain is almost zero for all values of Ω.

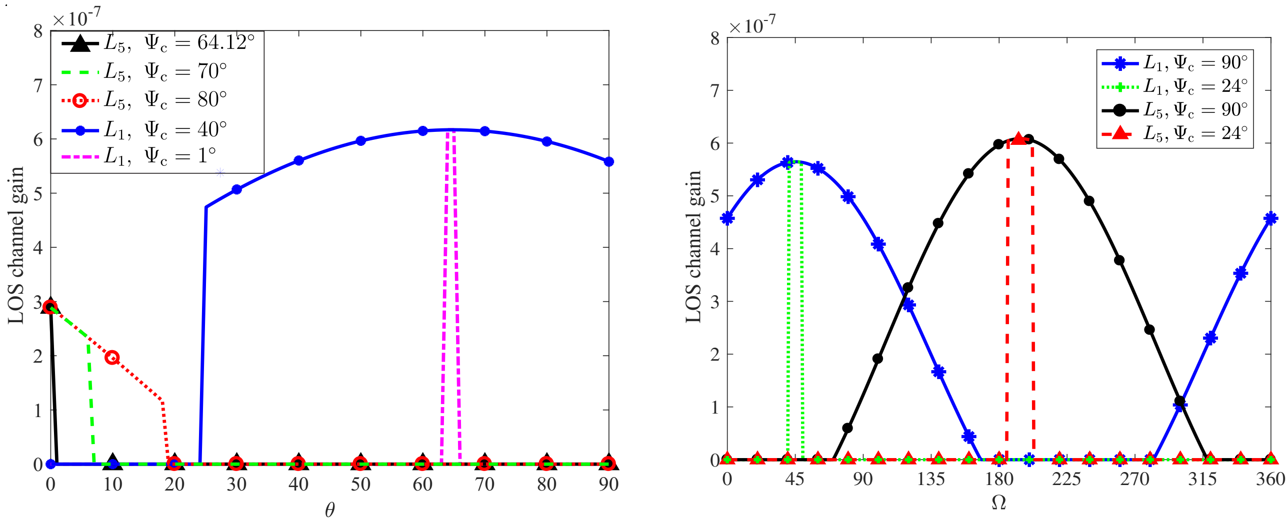

(a) $\Omega = 45°$

(b) $\theta = 41°$

Fig. 4: The effect of different FOVs on the LOS channel gain.

IV. Analysis of BER and Link Capacity

A. SNR Statistics

The received electrical SNR of OOK modulation in LiFi systems can be obtained as follows:

$$\mathcal{S} = \frac{R_{\mathrm{PD}}^2 H^2 P_{\mathrm{elec}}^2}{N_0 B}, \tag{9}$$

where R_{PD} represents the PD responsivity; P_{elec} denotes the transmitted electrical power. The single sided noise spectral density is N_0 and B is the modulation bandwidth. The channel gain, H, can be obtained by (1). Based on the experimental measurement of the device orientation reported in [13], the polar angle, θ, follows a truncated Laplace distribution between 0 and $\pi/2$ for sitting activities. For walking activities, the Gaussian distribution matches the experimental measurements more closely. The distribution of the LOS channel gain is reported to follow a clipped Laplace distribution as [13], [14]:

$$f_{\mathrm{H}}(\hbar) = \frac{\exp\left(-\frac{|\hbar - \mu_{\mathrm{H}}|}{b_{\mathrm{H}}}\right)}{b_{\mathrm{H}}\left(2 - \exp\left(-\frac{h_{\max} - \mu_{\mathrm{H}}}{b_{\mathrm{H}}}\right)\right)} + c_{\mathrm{H}}\delta(\hbar), \tag{10}$$

where the constant c_{H} is given as [14]:

$$\begin{aligned} c_{\mathrm{H}} &= F_{\cos\psi}(\cos\Psi_{\mathrm{c}}) \\ &\approx \begin{cases} 1 - \frac{1}{2}\exp\left(\frac{\theta_0 - \mu_\theta}{b_\theta}\right), & \theta_{\mathrm{ce}} < \mu_\theta \\ \frac{1}{2}\exp\left(-\frac{\theta_0 - \mu_\theta}{b_\theta}\right), & \theta_{\mathrm{ce}} \geq \mu_\theta \end{cases}, \end{aligned} \tag{11}$$

and $\theta_0 = \cos^{-1}\left(\frac{\cos\Psi_{\mathrm{c}}}{\sqrt{\lambda_1^2 + \lambda_2^2}}\right) + \tan^{-1}\left(\frac{\lambda_1}{\lambda_2}\right)$. The parameters μ_{H} and b_{H} are the mean and scaling factor of the LOS channel gain, respectively, which are given as:

$$\mu_{\mathrm{H}} = \frac{H_0}{d^{m+2}}\left(\lambda_1 \sin\mu_\theta + \lambda_2 \cos\mu_\theta\right), \tag{12}$$

$$b_{\mathrm{H}} = \frac{H_0}{d^{m+2}} b_\theta |\lambda_1 \cos\mu_\theta - \lambda_2 \sin\mu_\theta|, \tag{13}$$

where $H_0 = \frac{(m+1)Ah^m}{2\pi}$ and $b_\theta = \sqrt{\sigma_\theta^2/2}$. The factors, λ_1 and λ_2, are given in (4). The parameters μ_θ and σ_θ are the mean and standard deviation of the polar angle, which are obtained based on the experimental measurements. For static users, they are reported as $\mu_\theta = 41°$ and $\sigma_\theta = 7.3°$. The support range of $f_{\mathrm{H}}(\hbar)$, is $h_{\min} \leq \hbar \leq h_{\max}$ where $h_{\min}$ and $h_{\max}$ can be determined as:

$$h_{\min} = \begin{cases} \frac{H_0}{d^{m+2}} \cos\Psi_{\mathrm{c}}, & \cos\psi < \cos\Psi_{\mathrm{c}} \\ \frac{H_0}{d^{m+2}} \min\{\lambda_1, \lambda_2\}, & \text{o.w} \end{cases}, \tag{14}$$

$$h_{\max} = \begin{cases} \frac{H_0}{d^{m+2}} \lambda_2, & \text{if} \quad \lambda_1 < 0 \\ \frac{H_0}{d^{m+2}} \sqrt{\lambda_1^2 + \lambda_2^2}, & \text{if} \quad \lambda_1 \geq 0 \end{cases}. \tag{15}$$

Using the fundamental theorem of determining the distribution of a random variable [21], the probability density function (PDF) of SNR can be obtained as follows:

$$\begin{aligned} f_{\mathcal{S}}(s) &= \frac{f_H(\sqrt{s/\mathcal{S}_0})}{2\mathcal{S}_0\sqrt{s/\mathcal{S}_0}} \\ &= \frac{\exp\left(-\frac{|\sqrt{s} - \sqrt{\mathcal{S}_0}\mu_{\mathrm{H}}|}{\sqrt{\mathcal{S}_0} b_{\mathrm{H}}}\right)}{2b_{\mathrm{H}}\sqrt{\mathcal{S}_0 s}\left(2 - \exp\left(-\frac{h_{\max} - \mu_{\mathrm{H}}}{b_{\mathrm{H}}}\right)\right)} + c_{\mathrm{H}}\delta(s), \end{aligned} \tag{16}$$

where $\mathcal{S}_0 = \frac{R_{\mathrm{PD}}^2 P_{\mathrm{opt}}^2}{N_0 B}$ and with the support range of $s \in (s_{\min}, s_{\max})$, where $s_{\min} = \mathcal{S}_0 h_{\min}^2$ and $s_{\max} = \mathcal{S}_0 h_{\max}^2$, with $h_{\min}$ and $h_{\max}$ given in (14) and (15), respectively.

B. BER Performance

In this subsection, we aim to evaluate the effect of UE orientation on the BER performance of a LiFi-enabled device as one use case. The BER is one of the common metrics to evaluate point-to-point communication performance. Assuming the OOK modulation, the average BER of the communication link can be obtained as [22]:

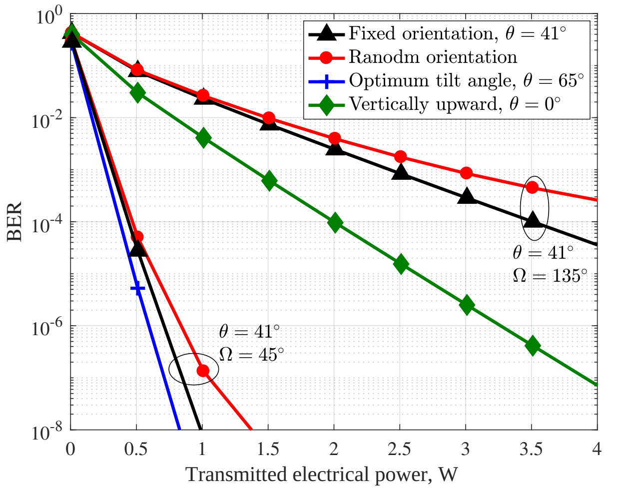

Fig. 5: Comparison of BER for different scenarios for UE's location of L_5.

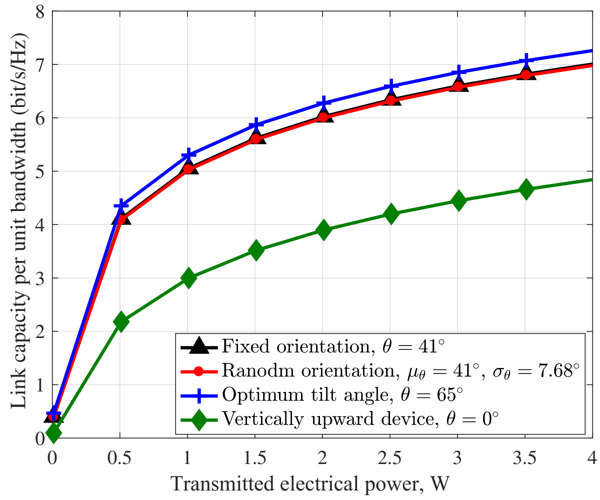

Fig. 6: Comparison of link capacity for random $\Omega = 45$ and 225.

$$\bar{P}_{\mathrm{e}} = \int_{s_{\min}}^{s_{\max}} Q\left(\sqrt{s}\right) f_S(s)\mathrm{d}s. \tag{17}$$

where $Q(\cdot)$ is the Q-function. Substituting (16) into (17) and calculating the integral from $s_{\min}$ to $s_{\max}$, we get the average BER of the OOK modulation for randomly-orientated UEs.

Fig. 5 represents a comparison of BER performance for four scenarios. First, a UE with a fixed orientation of $\theta = 41°$ and without any random orientation is considered. Second scenario is a UE with random orientation that the polar angle, θ, follows a Laplace model with mean and variance of $\mu_\theta = 41°$ and $\sigma_\theta = 7.68°$, respectively [13]. In the third scenario, the UE is assumed to be optimally tilted to the AP according to (6). Here, for the considered location of L_1, the optimum tilt angle is $\theta_{\mathrm{ot}} = 65°$. Finally, in the forth scenario, the UE is assumed to be vertically upward. As can be seen from these results, the fixed orientation scenario outperforms the random orientation one. The gap between these two scenarios becomes larger for higher SNRs. The reason for this is that in some cases with the random orientation the AP is out of the UE's FOV and hence an error floor is expected (see [14]). Therefore, after a certain point, extra transmitting power does not reduce the BER of the random orientation scenario. However, the BER of the fixed scenario decreases as the transmission power increases. The other interesting observation is the remarkable gap between the vertically upward scenario and random orientation one. This confirms the significance of considering the device random orientation in the analysis and performance evaluation. Finally, we note that the for any given location and direction of a UE, the minimum BER that can be achieved is for the optimum tilt angle, i.e., $\bar{P}_{\mathrm{e}} \leq Q\left(\sqrt{s_{\mathrm{ot}}}\right)$, where s_{ot} is the SNR corresponds to $\theta = \theta_{\mathrm{ot}}$. As shown in Fig. 5, the optimum tilt angle scenario has the minimum BER.

C. Upper Bound on Link Capacity

The upper bound of capacity in an additive white Gaussian noise (AWGN) channel is $C = B\log_2(1+s)$ based on the Shannon-Hartley theorem. However, with consideration of random orientation, this upper bound is given as:

$$C = \int_{s_{\min}}^{s_{\max}} \left(\frac{e^{-\frac{|\sqrt{s}-\sqrt{S_0}\mu_{\mathrm{H}}|}{\sqrt{S_0}b_{\mathrm{H}}}}}{\Delta\sqrt{s}} + c_{\mathrm{H}}\delta(s) \right) \log_2(1+s)\mathrm{d}s. \tag{18}$$

where $\Delta = 2B^{-1}b_{\mathrm{H}}\sqrt{S_0}\left(2-\exp\left(-\frac{h_{\max}-\mu_{\mathrm{H}}}{b_{\mathrm{H}}}\right)\right)$. Noting that $I = \int_{s_{\min}}^{s_{\max}} c_{\mathrm{H}}\delta(s)\log_2(1+s)\mathrm{d}s = 0$ (since if $s_{\min} > 0$, due to the delta function $I = 0$ and if $s_{\min} = 0$, $I = c_{\mathrm{H}}\log_2(1) = 0$). Therefore, the integral in (18) can be rewritten as (19) given at the top of next page. This integral does not have a closed form and can be obtained numerically.

Same scenarios described in previous subsection are considered here. As presented in Fig. 6, compared to the other scenarios, the optimum tilt angle scenario provides the maximum link capacity. This would be the upper bound on link capacity at the given location of L_1. As can be seen, the random orientation and fixed orientation scenarios have almost the same performance while the gap between them and vertically upward scenario is remarkable.

V. Conclusions and Future Works

In this paper, the effect of receiver orientation including both polar and azimuth angles on LOS channel gain in a LiFi system is studied. We derived the optimum tilt angle, which depends on both user's location and direction. The PDF of SNR is derived for OOK modulation. Then, using the derived PDF of SNR, the BER of OOK in an AWGN channel with the random orientation of the receiver is evaluated. It is shown that the random orientation effect can be neglected when the optimum tilt angle is chosen. Finally, we assessed the effect of random orientation on the Shannon-Hartley upper bound capacity.

$$C = \frac{2}{\Delta}\begin{cases} \displaystyle\int_{\sqrt{s_{\min}}}^{\sqrt{s_{\max}}} \exp\left(-\frac{s-\sqrt{\mathcal{S}_0}\mu_{\mathrm{H}}}{\sqrt{\mathcal{S}_0}b_{\mathrm{H}}}\right)\log_2(1+s^2)\mathrm{d}s, & \sqrt{\mathcal{S}_0}\mu_{\mathrm{H}} < \sqrt{s_{\min}} \\ \displaystyle\int_{\sqrt{s_{\min}}}^{\sqrt{\mathcal{S}_0}\mu_{\mathrm{H}}} \exp\left(\frac{s-\sqrt{\mathcal{S}_0}\mu_{\mathrm{H}}}{\sqrt{\mathcal{S}_0}b_{\mathrm{H}}}\right)\log_2(1+s^2)\mathrm{d}s + \int_{\sqrt{\mathcal{S}_0}\mu_{\mathrm{H}}}^{\sqrt{s_{\max}}} \exp\left(-\frac{s-\sqrt{\mathcal{S}_0}\mu_{\mathrm{H}}}{\sqrt{\mathcal{S}_0}b_{\mathrm{H}}}\right)\log_2(1+s^2)\mathrm{d}s, & \sqrt{s_{\min}} < \sqrt{\mathcal{S}_0}\mu_{\mathrm{H}} < \sqrt{s_{\max}} \end{cases} \quad (19)$$

ACKNOWLEDGMENT

Soltani acknowledges the School of Engineering for providing financial support. Haas and Safari gratefully acknowledge financial support from EPSRC under grant EP/L020009/1 (TOUCAN).

APPENDIX

PROOF OF (8)

For a given UE's location, the $\cos\psi$ can be expressed as:

$$\cos\psi = \kappa_1 \cos\left(\Omega - \tan^{-1}\left(\frac{y_{\mathrm{u}} - y_{\mathrm{a}}}{x_{\mathrm{u}} - x_{\mathrm{a}}}\right)\right) + \kappa_2, \quad (20)$$

where κ_1 and κ_2 are given as:

$$\kappa_1 = \frac{r}{d}\sin\theta, \quad \kappa_2 = \frac{h}{d}\cos\theta. \quad (21)$$

Since $\theta \in [0°, 90°]$, so $\kappa_1 \geq 0$ and $\kappa_2 \geq 0$. Thus, based on (20), we always have $\cos\psi \leq \kappa_1 + \kappa_2$ for any arbitrary value of Ω. Therefore, if $\Psi_{\mathrm{c}} \leq \cos^{-1}(\kappa_1 + \kappa_2) \triangleq \Psi_{\theta,\min}$, the LOS channel gain is zero for all Ω. On the other hand, we have:

$$\kappa_1 + \kappa_2 = \frac{r}{d}\sin\theta + \frac{h}{d}\cos\theta. \quad (22)$$

Let's define the auxiliary angle, $\beta = \sin^{-1}\left(\frac{r}{d}\right)$. Recalling that $d = \sqrt{r^2 + h^2}$, it is clear that $\frac{h}{d} = \cos\beta$. Replacing for $\frac{r}{d}$ and $\frac{h}{d}$ by $\sin\beta$ and $\cos\beta$, respectively, then, (22) can be expressed as:

$$\begin{aligned} \kappa_1 + \kappa_2 &= \sin\beta\sin\theta + \cos\beta\cos\theta \\ &= \cos(\beta - \theta). \end{aligned} \quad (23)$$

Hence, $\Psi_{\theta,\min} = \cos^{-1}(\kappa_1 + \kappa_2) = |\beta - \theta|$. Using the triangle rules, β can be denoted as $\beta = \tan^{-1}\left(\frac{r}{h}\right)$. Thus,

$$\Psi_{\theta,\min} = \cos^{-1}(\kappa_1 + \kappa_2) = |\tan^{-1}\left(\frac{r}{h}\right) - \theta|.$$

This completes the proof of (20).

REFERENCES

[1] Cisco, "Cisco Visual Networking Index: Global Mobile Data Traffic Forecast Update, 2016–2021 White Paper," *white paper at Cisco.com*, Mar. 2017.

[2] H. Haas, L. Yin, Y. Wang, and C. Chen, "What is LiFi?" *J. Lightw. Technol.*, vol. 34, no. 6, pp. 1533–1544, Mar. 2016.

[3] M. D. Soltani, X. Wu, M. Safari, and H. Haas, "Access Point Selection in Li-Fi Cellular Networks with Arbitrary Receiver Orientation," in *IEEE Int. Symp. Pers., Indoor Mobile Radio Commun. (PIMRC)*, Valencia, Spain, Sept 2016, pp. 1–6.

[4] M. D. Soltani, H. Kazemi, M. Safari, and H. Haas, "Handover Modeling for Indoor Li-Fi Cellular Networks: The Effects of Receiver Mobility and Rotation," in *IEEE Wireless Commun. Netw. Conf. (WCNC)*, San Fransisco, USA, March 2017, pp. 1–6.

[5] A. A. Purwita, M. D. Soltani, M. Safari, and H. Haas, "Handover Probability of Hybrid LiFi/RF-based Networks with Randomly-Oriented Devices," in *IEEE Veh. Technol. Conf. (VTC Spring)*, Porto, Portugal, June 2018.

[6] J. Y. Wang, Q. L. Li, J. X. Zhu, and Y. Wang, "Impact of Receiver's Tilted Angle on Channel Capacity in VLCs," *Electronics Letters*, vol. 53, no. 6, pp. 421–423, Mar. 2017.

[7] J. Y. Wang, J. B. Wang, B. Zhu, M. Lin, Y. Wu, Y. Wang, and M. Chen, "Improvement of BER Performance by Tilting Receiver Plane for Indoor Visible Light Communications with Input-Dependent Noise," in *IEEE Int. Conf. Commun. (ICC)*, Paris, France, May 2017, pp. 1–6.

[8] Z. Wang, C. Yu, W.-D. Zhong, and J. Chen, "Performance Improvement by Tilting Receiver Plane in M-QAM OFDM Visible Light Communications," *Optics Express*, vol. 19, no. 14, pp. 13 418–13 427, 2011.

[9] A. A. Matrawy, M. El-Shimy, M. Rizk, Z. El-Sahn *et al.*, "Optimum Angle Diversity Receivers for Indoor Single User MIMO Visible Light Communication Systems," in *Asia Communications and Photonics Conference*. Wuhan, China: Optical Society of America, 2016, pp. AS2C–4.

[10] Y. S. Eroglu, Y. Yapici, and I. Guvenc, "Impact of Random Receiver Orientation on Visible Light Communications Channel," *arXiv preprint arXiv:1710.09764*, 2017.

[11] A. A. Purwita, M. D. Soltani, M. Safari, and H. Haas, "Terminal Orientation in OFDM-based LiFi Systems," *arXiv preprint arXiv:1808.09269*, 2018.

[12] Z. Zeng, M. D. Soltani, H. Haas, and M. Safari, "Orientation Model of Mobile Device for Indoor Visible Light Communication and Millimetre Wave Systems," in *IEEE Veh. Technol. Conf. (VTC Fall)*, August.

[13] M. D. Soltani, A. A. Purwita, Z. Zeng, H. Haas, and M. Safari, "Modeling the Random Orientation of Mobile Devices: Measurement, Analysis and LiFi Use Case," *IEEE Trans. Commun.*, pp. 1–1, 2018.

[14] M. D. Soltani, A. A. Purwita, I. Tavakkolnia, H. Haas, and M. Safari, "Impact of Device Orientation on Error Performance of LiFi Systems," *arXiv preprint arXiv:1808.10476*, 2018.

[15] M. D. Soltani, M. A. Arfaoui, I. Tavakkolnia, A. Ghrayeb, M. Safari, C. Assi, M. Hasna, and H. Haas, "Bidirectional Optical Spatial Modulation for Mobile Users: Towards a Practical Design for LiFi Systems," *arXiv:1812.03109*, 2018.

[16] M. D. Soltani, X. Wu, M. Safari, and H. Haas, "Bidirectional User Throughput Maximization Based on Feedback Reduction in LiFi Networks," *IEEE Trans. Commun.*, vol. 66, no. 7, pp. 3172–3186, 2018.

[17] M. D. Soltani, M. Safari, and H. Haas, "On Throughput Maximization Based on Optimal Update Interval in Li-Fi Networks," in *IEEE Int. Symp. Pers., Indoor Mobile Radio Commun. (PIMRC)*. Montreal, QC, Canada: IEEE, Oct 2017, pp. 1–6.

[18] M. D. Soltani, X. Wu, M. Safari, and H. Haas, "On Limited Feedback Resource Allocation for Visible Light Communication Networks," in *Proceedings of the 2nd International Workshop on Visible Light Communications Systems*. Paris, France: ACM, Sept 2015, pp. 27–32.

[19] J. M. Kahn and J. R. Barry, "Wireless Infrared Communications," *Proc. IEEE*, vol. 85, no. 2, pp. 265–298, Feb. 1997.

[20] A. A. Purwita, M. D. Soltani, M. Safari, and H. Haas, "Impact of Terminal Orientation on Performance in LiFi Systems," in *IEEE Wireless Commun. Netw. Conf. (WCNC)*, Barcelona, Spain, April 2018.

[21] A. Papoulis and S. U. Pillai, *Probability, Random Variables, and Stochastic Processes and Queueing Theory*. Tata McGraw-Hill Education, 2002.

[22] Z. Ghassemlooy, W. Popoola, and S. Rajbhandari, *Optical Wireless Communications: System and Channel Modelling with Matlab*. CRC press, 2012.